

# Implementation of a 2D Panel Method for Potential Flow

Neslihan GULSOY\*

*Department of Aeronautical/Astronautical Engineering, Istanbul Technical University*

## Nomenclature

$\alpha$	=	angle of attack (deg)
$LE$	=	leading edge
$TE$	=	trailing edge
$c$	=	chord length ( $m$ )
$\gamma$	=	strength of vortex distribution
$q$	=	strength of source distribution
$\mu$	=	strength of doublet distribution
$Re$	=	Reynold number
$C_D$	=	drag coefficient
$C_L$	=	lift coefficient
$C_{m,c/4}$	=	moment coefficient around aerodynamic center
$\phi$	=	velocity potential ( $m^2/s$ )
$\phi_s \phi_v$	=	potential source and vortex ( $m^2/s$ )
$r$	=	distance of any field point ( $x, y$ ) measured from an arbitrary point, $b$ ( $m$ )
$\theta$	=	angle between panel and x axis ( $^\circ$ )
$ds$	=	length of panel ( $m$ )
$dx$	=	x component of $ds$ ( $m$ )
$dy$	=	y component of $ds$ ( $m$ )
$V_\infty$	=	free-stream velocity ( $m/s$ )
$N$	=	panel number
$\bar{n}, \bar{t}$	=	unit vector normal and tangential to panel surface
$(V^t)_i, (V^n)_i$	=	tangential and normal total velocity components at control point of $i - th$ panel

## I. Introduction

This paper is prepared as part of CA course and it contains a study on the 2 dimensional Hess-Smith panel method (HSPM) for a cambered airfoil, NACA 1408. Shape of airfoil is generated by an online tool. Panel coordinates are obtained by 4th degree polynomial curve fitting methods, then panel coordinates are used as input for HSPM algorithm. Outputs of HSPM algorithm is used to compute necessary aerodynamic coefficients. And then, obtained results are compared with experimental data to determine accuracy of HSPM. All calculation is conducted via MatLab.

This study showed that, the HSPM gives similar results with experimental data at relatively small angles of attack. However, the error rate increases with angle of attack, and HSPM is insufficient for angles exceeding the critical angle of attack.

## II. Panel Methods and Laplace's Equation

Laplace's equation is governing equation for inviscid, incompressible, irrotational flow. It is based on principle of incompressible mass conservation for an irrotational fluid. 2 dimensional Laplace's equation is given with [1],

$$\nabla^2 \phi = 0 \quad (1)$$

In 2D cylindrical coordinates it is [2],

$$\nabla^2 \phi = \frac{1}{r} \frac{\partial}{\partial r} \left( r \frac{\partial \phi}{\partial r} \right) + \frac{1}{r^2} \frac{\partial^2 \phi}{\partial \theta^2} = 0 \quad (2)$$

---

\*Undergraduate Student at ITU, Aerospace Engineering, gulsoy16@itu.edu.tr

Laplace's equation is an elliptic second order partial derivative equation so, there is no analytic, closed-form solution of this equation [3].

Panel methods aim to solve Laplace's equation numerically. For that, firstly airfoil surface are divided into several segments (panels). Then, constant or varying singularities are placed into those panels at control point. By boundary conditions, Laplace's equation is solved as a sum of all the singularity contributions in each panel.

Governing equation for 2D panel methods for the potential outside an arbitrary body given as [1],

$$\phi(P) = \phi_{\infty}(P) + \frac{1}{2\pi} \oint_{S_B} \left[ q \ln r - \mu \frac{\partial}{\partial n} \ln r \right] dS \quad (3)$$

Panel methods can be produced by following basic six step procedure [1].

#### Procedure for Panel Methods

1. Selection of singularity element
2. Discretization of geometry
3. Influence coefficients
4. Establish boundary conditions.
5. Solving linear algebraic equations.
6. Calculating of pressure and loads.

Even there are various panel methods, in this paper only Hess-Smith panel method will be examined.

### III. Hess-Smith Panel Method

This section of paper contains derivation of Hess-Smith panel algorithm.

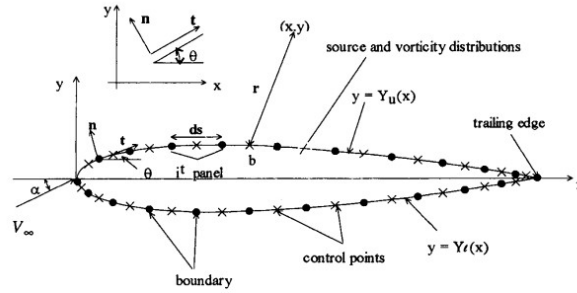


Fig. 1 Panel Representation [4]

Considering an airfoil under a steady, incompressible and inviscid flow. From Fig. 1 normal and tangential direction from body into the fluid can be written as,

$$\bar{n} = -\sin\theta\bar{i} + \cos\theta\bar{j} \quad (4a)$$

$$\bar{t} = \cos\theta\bar{i} + \sin\theta\bar{j} \quad (4b)$$

Also, relation between length of panel is,

$$dx = \cos\theta ds, \quad dy = \sin\theta ds \quad (5)$$

#### 1. Selection of Singularity Element

HSPM uses varying source and constant vortex singularities on each panel. After discretization of the surface of the bodies and changing doublet singularities with constant vortex, Eq. 3 becomes,

$$\phi(P') = \phi_{\infty} + \sum_{j=1}^N \int_{\text{panel } j} \left[ \frac{q(s)}{2\pi} \ln r - \frac{\gamma(s)}{2\pi} \theta \right] dS \quad (6)$$

where  $\phi_\infty = V_\infty(x\cos\alpha + y\sin\alpha)$ .

Normal and tangential velocity components at panel control points are given with,

$$(V^n)_i = \sum_{j=1}^N A_{ij}^n q_j + \sum_{j=1}^N B_{ij}^n \gamma + V_\infty \sin(\alpha - \theta_i) \quad (7a)$$

$$(V^t)_i = \sum_{j=1}^N A_{ij}^t q_j + \sum_{j=1}^N B_{ij}^t \gamma + V_\infty \cos(\alpha - \theta_i) \quad (7b)$$

where  $A_{ij}^n$  and  $A_{ij}^t$  are normal and tangential velocity components induced at the  $i$ -th panel control point by a unit strength source distribution on the  $j$ -th panel respectively.  $B_{ij}^n$  and  $B_{ij}^t$  are normal and tangential velocity components induced at the  $i$ -th panel control point by a unit strength vorticity distribution on the  $j$ -th panel respectively.

## 2. Discretization of Geometry

It is customary to use the cosine spacing function to create more panels near LE and TE. This function is given with [1],

$$\frac{x_i}{c} = \frac{1}{2} \left[ 1 - \cos \frac{(i-1)\pi}{N-1} \right], \quad i = 1, \dots, N \quad (8)$$

After  $x$  axis divided into  $N$  panels,  $N+1$  corner points are obtained. Noted that, numbering begins from trailing edge of bottom surface and ends at trailing edge of upper surface. The control (i.e., collocation) points are placed at the center of each panel.

## 3. Influence coefficients

Influence coefficients represent the contribution of singularity elements on  $j$ -th panel to induced velocity at  $i$ -th panel and they are given with [4],

$$A_{ij}^n = \begin{cases} \frac{1}{2\pi} \left[ \sin(\theta_i - \theta_j) \ln \frac{r_{i,j+1}}{r_{i,j}} + \cos(\theta_i - \theta_j) \beta_{ij} \right] & i \neq j \\ \frac{1}{2} & i = j \end{cases} \quad (9)$$

$$A_{ij}^t = \begin{cases} \frac{1}{2\pi} \left[ \sin(\theta_i - \theta_j) \beta_{ij} - \cos(\theta_i - \theta_j) \ln \frac{r_{i,j+1}}{r_{i,j}} \right] & i \neq j \\ \frac{1}{2} & i = j \end{cases} \quad (10)$$

$$B_{ij}^n = -A_{ij}^t \quad B_{ij}^t = A_{ij}^n \quad (11)$$

where,

$$r_{i,j+1} = [(x_{m_i} - x_{j+1})^2 + (y_{m_i} - y_{j+1})^2]^{1/2} \quad (12a)$$

$$r_{i,j} = [(x_{m_i} - x_j)^2 + (y_{m_i} - y_j)^2]^{1/2} \quad (12b)$$

$$x_{m_i} = \frac{1}{2}(x_i + x_{i+1}), \quad y_{m_i} = \frac{1}{2}(y_i + y_{i+1}) \quad (12c)$$

$$\theta_i = \tan^{-1} \left( \frac{y_{i+1} - y_i}{x_{i+1} - x_i} \right), \quad \theta_j = \tan^{-1} \left( \frac{y_{j+1} - y_j}{x_{j+1} - x_j} \right) \quad (12d)$$

$$\beta_{ij} = \tan^{-1} \left( \frac{y_{m_i} - y_{j+1}}{x_{m,i} - x_{j+1}} \right) - \tan^{-1} \left( \frac{y_{m_i} - y_j}{x_{m,i} - x_j} \right) \quad (12e)$$

## 4. Establishing Boundary Conditions

The induced velocities must satisfy the irrotationality condition and the boundary condition at infinity

$$u = \frac{\partial \phi}{\partial x} = V_\infty \cos \alpha \quad (13a)$$

$$v = \frac{\partial \phi}{\partial y} = V_\infty \sin \alpha \quad (13b)$$

Also surface of the body is a streamline of flow. So, on surface boundary condition is,

$$\frac{\partial \phi}{\partial n} = 0 \quad (14)$$

Eq. 14 asserts that sum of induced velocities and freestream velocity must be set to zero in normal direction of surface. It is also known as flow tangency condition. So flow tangency condition is written by recalling Eq. 7a,

$$(V^n)_i = \sum_{j=1}^N A_{ij}^n q_j + \sum_{j=1}^N B_{ij}^n \gamma + V_\infty \sin(\alpha - \theta_i) = 0 \quad (15)$$

The Kutta condition must also be satisfied, which asserts that the flow leaves the trailing edge smoothly. This condition can be written as,

$$(V^t)_N = -(V^t)_1 \quad (16a)$$

$$\sum_{j=1}^N A_{1j}^t q_j + \gamma \sum_{j=1}^N B_{1j}^t + V_\infty \cos(\alpha - \theta_1) = - \left[ \sum_{j=1}^N A_{Nj}^t q_j + \gamma \sum_{j=1}^N B_{Nj}^t + V_\infty \cos(\alpha - \theta_N) \right] \quad (16b)$$

### 5. Solving Linear Algebraic Equations

System contains  $N + 1$  unknown strengths of singularities,  $q_1, \dots, q_N, \gamma$ . To find unknowns,  $N$  flow tangency equations and 1 Kutta's condition on trailing edge are written with Eq. 15 and Eq. 16. So, linear algebraic equation are given form of  $Ax = b$ .

$$\begin{bmatrix} a_{1,1} & \dots & a_{1,j} & \dots & a_{1,N} & a_{1,N+1} \\ \vdots & \vdots & \vdots & \dots & \vdots & \vdots \\ a_{N,1} & \dots & a_{N,j} & \dots & a_{N,N} & a_{N,N+1} \\ a_{N+1,1} & \dots & a_{N+1,j} & \dots & a_{N+1,N} & a_{N+1,N+1} \end{bmatrix} \begin{bmatrix} q_1 \\ \vdots \\ q_N \\ \gamma \end{bmatrix} = \begin{bmatrix} -V_\infty \sin(\alpha - \theta_1) \\ \vdots \\ -V_\infty \sin(\alpha - \theta_N) \\ -V_\infty \cos(\alpha - \theta_1) - V_\infty \cos(\alpha - \theta_N) \end{bmatrix} \quad (17)$$

where,

$$a_{ij} = A_{ij}^n \quad (18a)$$

$$a_{i,N+1} = \sum_{j=1}^N B_{ij}^n \quad (18b)$$

$$a_{N+1,j} = A_{1j}^t + A_{Nj}^t \quad (18c)$$

$$a_{N+1,N+1} = \sum_{j=1}^N (B_{1j}^t + B_{Nj}^t) \quad (18d)$$

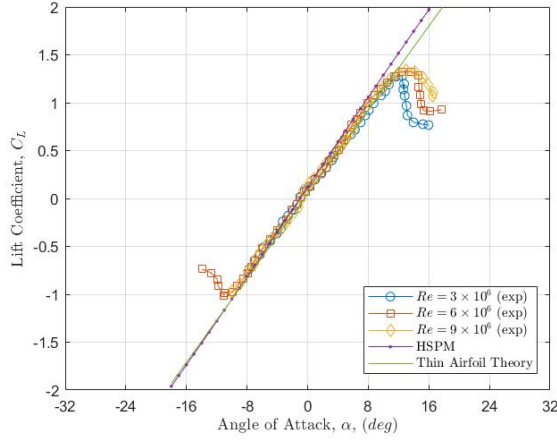
### 6. Calculation of Pressure and Loads

After strengths of singularities are found, the tangential velocity component at each collocation point are written with Eq. 7b. Noted that, tangential component is equal to the total velocity as the normal components are set to zero due to the flow tangency condition. From Bernoulli's equation pressure coefficient at each panel is,

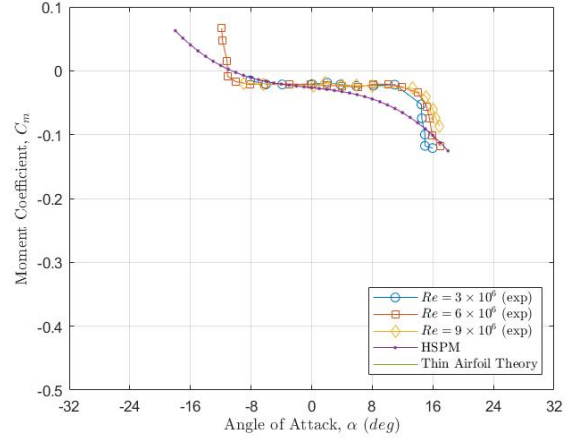
$$C_{p,i} = 1 - \left( \frac{V_i^t}{V_\infty} \right)^2 \quad (19)$$

## IV. Comparison with Experimental Data& Conclusion

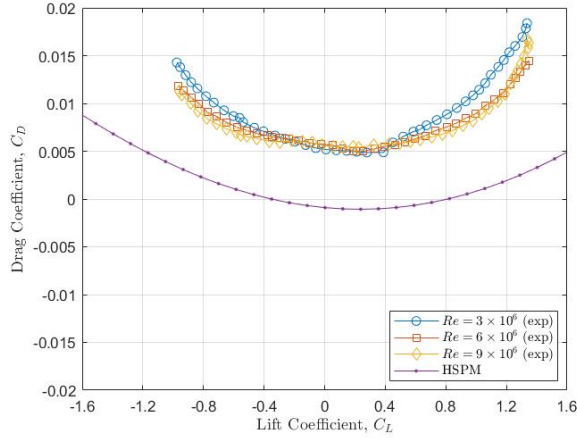
HSPM is written in MatLab environment. Written code is applied at a cambered airfoil, NACA1408. Panel number is set to 200 and characteristic coefficients are found under varying free-stream and angle of attack.



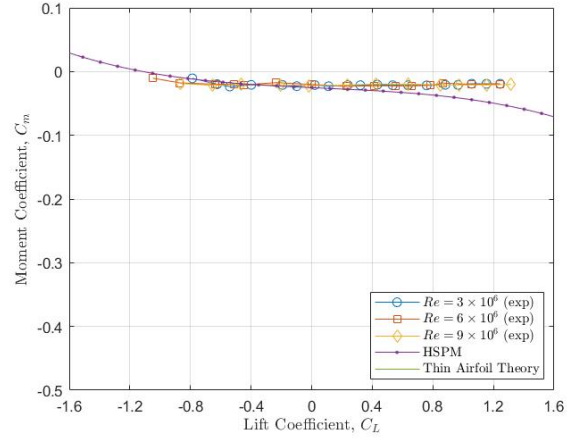
(a) Lift Coefficient Comparison



(b) Moment Coefficient Comparison



(c) Drag versus Lift Coefficients Comparison



(d) Moment versus Lift Coefficients Comparison

**Fig. 2 Comparison of Aerodynamic Characteristic of NACA 1408**

$\alpha$ (deg)	Lift Coefficient $C_L$				
	Thin Airfoil Theory	HSPM	Experimental Data		
			Re = $3 \times 10^6$	Re = $6 \times 10^6$	Re = $9 \times 10^6$
-16	-1.7092	-1.7364	NaN		
-8	-0.8319	-0.8079	$\approx -0.78$		
-4	-0.3933	-0.3440	$\approx -0.34$		
0	0.0454	0.1218	$\approx 0.1$		
4	0.4840	0.5871	$\approx 0.54$		
8	0.9227	1.0495	$\approx 0.96$		
16	1.8000	1.9567	$\approx 0.8$	$\approx 0.9$	$\approx 1.2$

**Table 1 Comparison of Lift Coefficient**

To investigate the limit and accuracy of HSPM, obtained results are compared with experimental data for NACA 1408 and analytical results by thin airfoil theory. Fig. 2 represents this comparative study. Experimental data are obtained from Ref. [5] by a digitizer program Ref. [6].

As seen in Fig. 2a and Tab. 1 the HSPM gives results for lift coefficient with error of  $\approx 7\%$  at relatively small angles of attack, i.e. in the range of  $\alpha \pm 6^\circ$ . Although this error rate is not at the desired level, it is acceptable considering the simplicity of the numeric method.

However, as the angle of attack increases, the error rate continues to increase and approaches after a certain angle

range. Limits of this range is called as critical angle of attack and it is approximately  $\alpha = -15^\circ$  and  $\alpha = 16^\circ$  for NACA 1408. When this limits are exceeded, the airplane is in a stall condition and HSPM is no longer usable.

On the other hand when Fig. 2b is examined it is seen that,  $C_{m,c/4}$  calculated with HSPM varies with angle of attack. Error varies with angle of attack and maximum error is calculated as 60%. But it is still better than thin-airfoil theory. As seen in Fig. 2c, HSPM is not sufficient to compute drag.

When considering only thin-airfoil theory and HSPM, it can be said that, HSPM gives same results for varying free-stream and lift coefficient shows a linear behavior similar with thin airfoil theory. But, unlike the thin airfoil theory, in HSPM the pressure distribution over the airfoil is calculated. characteristic coefficients are found with the help of this calculated pressure distribution. So while the thin-airfoil theory says nothing about drag and also the moment coefficient is considered constant, these coefficients can be calculated for varying angle of attacks by HSPM.

As a conclusion, HSPM, which was derived in 60's decade of the last century, is still used frequently today to compute airfoil characteristic. The accuracy of the method depends on the accuracy of potential flow assumption. To test accuracy and limits of HSPM, it is applied for a chambered airfoil NACA 1408.

With all the above results, the following conclusions can be drawn, HSPM lack the ability to model stall conditions. Error when stall occurs, reaches to  $\infty$ . Because the HSPM is based on potential flow assumption, as known viscous effect increases with angle of attack. Also, HSPM can not correctly infer about drag. Although, HSPM is still useful than thin-airfoil theory and it can be preferred for small angle of attack due to it's simplicity.

## References

- [1] Katz, J., and Plotkin, A., *Low-Speed Aerodynamics*, 2<sup>nd</sup> ed., Cambridge Aerospace Series, Cambridge University Press, 2001. <https://doi.org/10.1017/CBO9780511810329>.
- [2] Anderson, J., *Fundamentals of Aerodynamics*, 5<sup>th</sup> ed., McGraw-Hill, 2011.
- [3] Cummings, R. M., Mason, W. H., Morton, S. A., and McDaniel, D. R., *Applied Computational Aerodynamics: A Modern Engineering Approach*, Cambridge University Press, 2015. <https://doi.org/10.1017/CBO9781107284166>.
- [4] Cebeci, T., Platzer, M., Chen, H., Chang, K.-C., and Shao, J. P., *Analysis of Low-Speed Unsteady Airfoil Flows*, Springer Berlin Heidelberg, 2005. <https://doi.org/10.1007/b138967>.
- [5] Abbott, I. H., Doenhoff, A. E. V., and Stivers, L. S., "Report No. 824 - Summary of Airfoil Data," , n.d. URL <https://engineering.purdue.edu/~aerodyn/AAE514/Spring%202011/naca-report-824.pdf>.
- [6] "WebPlotDigitizer - Copyright 2010-2022 Ankit Rohatgi," , n.d. URL <https://apps.automeris.io/wpd/>.